Mechanism of the quasi-zero axial acoustic radiation force experienced by elastic and viscoelastic spheres in the field of a quasi-Gaussian beam and particle tweezing

F. G. Mitri, Zine El Abiddine Fellah

Mechanism of the quasi-zero axial acoustic radiation force experienced by elastic and viscoelastic spheres in the field of a quasi-Gaussian beam and particle tweezing

F.G. Mitri[†], Z.E.A. Fellah*

[†]Los Alamos National Laboratory, MPA-11, Sensors & Electrochemical Devices, Acoustics & Sensors Technology Team, MS D429, Los Alamos, NM 87545, USA

*Laboratoire de Mécanique et d'Acoustique, CNRS-UPR 7051, 31 chemin Joseph Aiguier, Marseille, 13402, France.

Corresponding author:

F.G. Mitri, emails: mitri@ieee.org, mitri@lanl.gov

Abstract – The present analysis investigates the (axial) acoustic radiation force induced by a quasi-Gaussian beam of progressive (traveling) waves centered on an elastic and a viscoelastic (polymer-type) sphere in a nonviscous fluid. The quasi-Gaussian beam is an exact solution of the source free Helmholtz wave equation and is characterized by an arbitrary waist w_0 and a diffraction convergence length known as the Rayleigh range z_R. Examples are found where the radiation force unexpectedly approaches closely to zero at some of the elastic sphere's resonance frequencies for $kw_0 \leq 1$ (where this range is of particular interest in describing strongly focused or divergent beams), which may produce particle immobilization along the axial direction. Moreover, the (quasi)vanishing behavior of the radiation force is found to be correlated with conditions giving extinction of the backscattering by the quasi-Gaussian beam. Furthermore, the mechanism for the quasi-zero force is studied theoretically by analyzing the contributions of the kinetic, potential and momentum flux energy densities and their density functions. It is found that all the components vanish simultaneously at the selected *ka* values for the nulls. However, for a viscoelastic sphere, acoustic absorption degrades the quasi-zero mean force.

1. Introduction

Quasi-Gaussian beams have been recently originated in the wave diffraction theory as an exact solution of the Helmholtz equation. The properties of such beams have been analyzed from the standpoint of the classical wave propagation theory based on the complex source point method [1-8] to obtain the expression of the pressure for the incident quasi-Gaussian beam, and expand it using a partial-wave series [9, 10]. A quasi-Gaussian beam (Fig. 1) is characterized by an arbitrary waist w_0 and a diffraction convergence length known as the Rayleigh range z_R. Moreover, the beam has the form of a superposition of sources and sinks with complex coordinates [9].

In a recent investigation [11], the scattering (which is an important phenomenon in many applications, for example nondestructive imaging applications [12, 13], medical imaging etc.), instantaneous and mean radiation forces experienced by a rigid and immovable (fixed) sphere centered on the axis of the beam have been investigated theoretically. Situations have been observed where significant differences have occurred between the quasi-Gaussian beam and the plane wave results for $kw_0 < 25$, (where k denotes the wavenumber of the incident beam), however, the plane wave results have been recovered when $kw_0 > 25$ and increases toward $\rightarrow \infty$.

The purpose here is to illustrate situations where the radiation force function (which the radiation force per unit energy density and unit cross-section) tends to zero at some of the resonance frequencies of an *elastic* sphere and specific values of kw_0. The formalism for the scattering derived previously [11] is used here to evaluate the acoustic radiation force of a quasi-Gaussian beam on an elastic sphere in a nonviscous fluid, and correlate the backscattering and radiation force function plots. Moreover, the mechanism for the

quasi-zero force is studied theoretically by analyzing the contributions of the kinetic, potential and momentum flux energy densities and their density functions. Additional examples are provided for a (polymer-type) viscoelastic sphere. The extension of the previous work [11] to account for the sphere's elasticity may be helpful for the identification of some conditions where ultrasonic quasi-Gaussian beams may be used to immobilize a sphere (or a spherical shell, a layered sphere [14-16], or a layered spherical shell [17]) in a fluid with negligible viscosity. It is important to identify such conditions using *a priori* information obtained from theoretical predictions since it may be experimentally easier to verify the existence of zero acoustic radiation forces in quasi-Gaussian beams using solid objects.

2. Radiation force, its components and density functions

The mean (time-averaged) radiation force of a quasi-Gaussian beam of continuous waves is expressed as [18, 19],

$$\left\langle \mathbf{F}_{rad} \right\rangle = \iint_{S_0} \left\langle \mathscr{L} \right\rangle \mathbf{n}\, dS - \iint_{S_0} \left\langle \rho\, \mathbf{v}^{(1)} \left(\mathbf{v}^{(1)} \cdot \mathbf{n} \right) \right\rangle dS, \tag{1}$$

where,

$$\begin{aligned} \mathscr{L} &= \frac{\rho_0}{2} \left| \mathbf{v}^{(1)} \right|^2 - \frac{1}{2\rho_0 c_0^2}\, p^{(1)^2} \\ &= \mathscr{K} - \mathscr{U}, \end{aligned} \tag{2}$$

is the Lagrangean energy density, the superscript $^{(1)}$ denotes first-order quantities, $\mathbf{v}^{(1)} = \nabla \varphi$, $p^{(1)} = -\rho_0 \dfrac{\partial \varphi^{(1)}}{\partial t}$, and $\varphi^{(1)} = \mathrm{Re}\left[\Phi^{(1)} \right]$, where $\Phi^{(1)}$ is the total (incident +

scattered) linear velocity potential that is related to the total pressure in the surrounding fluid.

This equation can be rewritten in terms of the following factors [20],

$$\langle \mathbf{F}_{rad} \rangle = \iint_{S_0} \langle \mathscr{K} \rangle \mathbf{n}\, dS - \iint_{S_0} \langle \mathscr{Q} \rangle \mathbf{n}\, dS - \iint_{S_0} \langle \mathscr{P} \rangle dS, \tag{3}$$

where $\mathscr{P} = \rho_0 \mathbf{v}^{(1)} v_n^{(1)}$, is the momentum flux energy density, and $v_n^{(1)}$ is the normal component of the velocity. The three components of the radiation force on an elastic sphere can be represented in terms of the total velocity potential $\Phi^{(1)}$ given by the partial-wave series as,

$$\varphi^{(1)} = \mathrm{Re}\left[\Phi^{(1)} \right] = \sum_{n=0}^{\infty} \Phi_0 \left(2n+1\right) R_n P_n \left(\cos\theta\right), \tag{4}$$

where, Φ_0 is the amplitude. The coefficient R_n is given by [11],

$$R_n = \mathrm{Re}\left[i^n \left(U_n \left(kr\right) + iV_n \left(kr\right) \right) g_n \left(kz_R\right) e^{-i\omega t} \right], \tag{5}$$

and,

$$\begin{aligned} U_n &= \left(1+\alpha_n\right) j_n \left(kr\right) - \beta_n y_n \left(kr\right), \\ V_n &= \beta_n j_n \left(kr\right) + \alpha_n y_n \left(kr\right), \end{aligned} \tag{6}$$

where $y_n(.)$ are the spherical Neumann functions (or the spherical Bessel functions of the second kind), $\alpha_n = \mathrm{Re}\left[S_n\right]$, $\beta_n = \mathrm{Im}\left[S_n\right]$, and S_n are the scattering coefficients determined by applying appropriate boundary conditions at the interface fluid-structure, with the assumption that the surrounding fluid is nonviscous. These functions depend on the sphere's elastic parameters such as the longitudinal c_L, the shear or transverse c_T sound speed and the mass densities of both the fluid ρ_0 and the sphere ρ_s. It should be

emphasized that those coefficients are found equivalent to those obtained from the study of acoustic scattering by plane waves (See Appendix in [21]).

The three components of the radiation force are now expressed as [20],

$$\begin{aligned}\iint_{S_0}\left\langle \mathscr{X}\right\rangle \mathbf{n}\,dS &= \pi\rho_0 a^2\left(\frac{1}{a^2}\int_0^{\pi}\left\langle\left(\frac{\partial\Phi^{(1)}}{\partial\theta}\right)^2_{r=a}\right\rangle\sin\theta\cos\theta\,d\theta+\int_0^{\pi}\left\langle\left(\frac{\partial\Phi^{(1)}}{\partial r}\right)^2_{r=a}\right\rangle\sin\theta\cos\theta\,d\theta\right)\\ &= 2\pi\rho_0\left|\Phi_0\right|^2\sum_{n=0}^{\infty}\left\{g_n\left(kz_R\right)g_{n+1}\left(kz_R\right)\left(n+1\right)\begin{bmatrix}n\left(n+2\right)\left(V_nU_{n+1}-U_nV_{n+1}\right)\\+\left(ka\right)^2\left(V_n'U_{n+1}'-U_n'V_{n+1}'\right)\end{bmatrix}\right\}_{r=a},\end{aligned} \tag{7}$$

$$\begin{aligned}\iint_{S_0}\left\langle \mathscr{Y}\right\rangle \mathbf{n}\,dS &= \frac{\pi\rho_0 a^2}{c_0^2}\int_0^{\pi}\left\langle\left(\frac{\partial\Phi^{(1)}}{\partial t}\right)^2_{r=a}\right\rangle\sin\theta\cos\theta\,d\theta\\ &= 2\pi\rho_0\left|\Phi_0\right|^2\left(ka\right)^2\sum_{n=0}^{\infty}\left\{g_n\left(kz_R\right)g_{n+1}\left(kz_R\right)\left(n+1\right)\left(V_nU_{n+1}-U_nV_{n+1}\right)\right\}_{r=a},\end{aligned} \tag{8}$$

$$\begin{aligned}\iint_{S_0}\left\langle \mathscr{R}\right\rangle dS &= -2\pi\rho_0 a^2\left(\frac{1}{a}\int_0^{\pi}\left\langle\left(\frac{\partial\Phi^{(1)}}{\partial r}\right)_{r=a}\left(\frac{\partial\Phi^{(1)}}{\partial\theta}\right)_{r=a}\right\rangle\sin^2\theta\,d\theta+\int_0^{\pi}\left\langle\left(\frac{\partial\Phi^{(1)}}{\partial r}\right)^2_{r=a}\right\rangle\sin\theta\cos\theta\,d\theta\right)\\ &= -2\pi\rho_0 ka\left|\Phi_0\right|^2\sum_{n=0}^{\infty}\left\{\begin{matrix}g_n\left(kz_R\right)g_{n+1}\left(kz_R\right)\left(n+1\right)\\ \times\begin{bmatrix}n\left(V_nU_{n+1}'-U_nV_{n+1}'\right)-\left(n+2\right)\left(V_n'U_{n+1}-U_n'V_{n+1}\right)\\-2\left(ka\right)\left(V_n'U_{n+1}'-U_n'V_{n+1}'\right)\end{bmatrix}\end{matrix}\right\}_{r=a}.\end{aligned} \tag{9}$$

Denoting by $E=\rho k^2\left|\Phi_0\right|^2/2$ the characteristic energy density, the axial time-averaged radiation force of a quasi-Gaussian beam is expressed by [11],

$$\left\langle F_{z,rad}\right\rangle = Y_{qG}S_cE, \tag{10}$$

where $S_c=\pi a^2$ is the cross-sectional area, and Y_{qG} is the radiation force function, which is the radiation force per unit energy density and unit cross-sectional surface given by [11],

$$Y_{qG} = -\frac{4}{(ka)^2}\sum_{n=0}^{\infty}\left\{g_n(kz_R)\,g_{n+1}(kz_R)(n+1)\left[\alpha_n + \alpha_{n+1} + 2\left(\alpha_n\alpha_{n+1} + \beta_n\beta_{n+1}\right)\right]\right\}. \tag{11}$$

In the same manner, the form functions for the kinetic energy density K_{qG}, potential energy density U_{qG} and momentum flux density R_{qG} are defined as,

$$\begin{aligned} K_{qG} &= \frac{\iint_{S_0}\langle \mathscr{K}\rangle \mathbf{n}\,dS}{\pi a^2 E} \\ &= \frac{4}{(ka)^2}\sum_{n=0}^{\infty}\left[g_n(kz_R)\,g_{n+1}(kz_R)(n+1)\left\{n(n+2)\left(V_nU_{n+1} - U_nV_{n+1}\right) + (ka)^2\left(V_n'U_{n+1}' - U_n'V_{n+1}'\right)\right\}\right]_{r=a}, \end{aligned} \tag{12}$$

$$\begin{aligned} U_{qG} &= -\frac{\iint_{S_0}\langle \mathscr{U}\rangle \mathbf{n}\,dS}{\pi a^2 E} \\ &= -4\sum_{n=0}^{\infty}\left\{g_n(kz_R)\,g_{n+1}(kz_R)(n+1)\left(V_nU_{n+1} - U_nV_{n+1}\right)\right\}_{r=a}, \end{aligned} \tag{13}$$

$$\begin{aligned} R_{qG} &= -\frac{\iint_{S_0}\langle \mathscr{R}\rangle dS}{\pi a^2 E} \\ &= \frac{4}{(ka)}\sum_{n=0}^{\infty}\left\{g_n(kz_R)\,g_{n+1}(kz_R)(n+1)\begin{bmatrix} n\left(V_nU_{n+1}' - U_nV_{n+1}'\right) - (n+2)\left(V_n'U_{n+1} - U_n'V_{n+1}\right) \\ -2(ka)\left(V_n'U_{n+1}' - U_n'V_{n+1}'\right)\end{bmatrix}\right\}_{r=a}, \end{aligned} \tag{14}$$

so the radiation force function is rewritten as,

$$Y_{qG} = K_{qG} + U_{qG} + R_{qG}. \tag{15}$$

To further calculate the radiation force function's distribution versus the polar angle θ over the sphere's surface at a particular dimensionless frequency ka, a density function $y_{qG}(\theta)$ is defined for Y_{qG} as,

$$Y_{qG} = \int_0^{\pi} y_{qG}(\theta)\,d\theta. \tag{16}$$

The density function $y_{qG}(\theta)$ physically represents the contribution of the radiation force function along a certain direction θ. Following Eq.(16), the kinetic $k_{qG}(\theta)$, potential $u_{qG}(\theta)$ and momentum flux $r_{qG}(\theta)$ density functions are defined as,

$$K_{qG} = \int_0^{\pi} k_{qG}(\theta)\, d\theta, \tag{17}$$

$$U_{qG} = \int_0^{\pi} u_{qG}(\theta)\, d\theta, \tag{18}$$

$$R_{qG} = \int_0^{\pi} r_{qG}(\theta)\, d\theta. \tag{19}$$

The density form functions are expressed as,

$$k_{qG}(\theta) = \frac{\rho_0}{E}\left(\frac{1}{a^2}\left\langle\left(\frac{\partial\Phi^{(1)}}{\partial\theta}\right)^2_{r=a}\right\rangle + \left\langle\left(\frac{\partial\Phi^{(1)}}{\partial r}\right)^2_{r=a}\right\rangle\right)\sin\theta\cos\theta, \tag{20}$$

$$u_{qG}(\theta) = -\frac{\rho_0}{c_0^2 E}\left\langle\left(\frac{\partial\Phi^{(1)}}{\partial t}\right)^2_{r=a}\right\rangle\sin\theta\cos\theta, \tag{21}$$

$$r_{qG}(\theta) = 2\frac{\rho_0}{E}\left(\frac{1}{a}\left\langle\left(\frac{\partial\Phi^{(1)}}{\partial r}\right)_{r=a}\left(\frac{\partial\Phi^{(1)}}{\partial\theta}\right)_{r=a}\right\rangle\sin^2\theta - \left\langle\left(\frac{\partial\Phi^{(1)}}{\partial r}\right)^2_{r=a}\right\rangle\sin\theta\cos\theta\right). \tag{22}$$

Using the identity for the time-average of a product of two complex functions (p. 25-26 in [22]), Eqs.(20)-(22) can be directly evaluated at $r = a$ using Eqs.(4)-(6), so that the density function $y_{qG}(\theta)$ for Y_{qG} is expressed as,

$$y_{qG}(\theta) = k_{qG}(\theta) + u_{qG}(\theta) + r_{qG}(\theta). \tag{23}$$

3. Numerical results, discussion and concluding remarks

The following examples are considered to illustrate the theory by plotting the radiation force function Y_{qG} for acoustical quasi-Gaussian beam incident upon elastic and viscoelastic spheres immersed in water (ρ_{water} = 1060 kg/m^3, c_{water} = 1470 m/s). In addition, the magnitude of the backscattering form-function $\left|f_\infty\left(ka, kz_R, \pi\right)\right|$, (Eq.(8) in [11]) is displayed to correlate the radiation force function plots with the backscattering. The simulations are evaluated in the dimensionless frequency range $0 < ka \leq 10$ for selected values of the dimensionless beam waist parameter kw_0 at which the quasi-zero behavior in the Y_{qG} plots is manifested.

The top and bottom panels in Figure 2 show the plots for the backscattering form-function (Eq.(8) in [11]) and radiation force function (Eq.(11)), respectively, for a polymethylmetacrylate (PMMA) *elastic* sphere (ρ_{PMMA} = 1191 kg/m^3, $c_{L,PMMA}$ = 2690 m/s, $c_{T,PMMA}$ = 1340 m/s) for $kw_0 = 0.1$ (solid line), $kw_0 = 1$ (long-dashed line), $kw_0 = 1.5$ (dashed-dotted line), and $kw_0 = 2$ (dotted line). The arrows along the *ka* axis in the bottom panel point to the zeros of Y_{qG} that occur at the minima-resonances of the elastic sphere. Visual inspection and comparison of both curves indicate the correlation of the quasi-zero radiation force with the reduction in the backscattering direction; the nulls in the plots for $\left|f_\infty\left(ka, kz_R, \pi\right)\right|$ closely match those of Y_{qG} for $kw_0 \leq 1$. At those specific *ka* values that correspond to nulls, the transmission of sound waves through the elastic sphere in the forward direction (i.e. axial direction $\theta = 0$) is total. Moreover, as explained in [9], this range of $kw_0 \leq 1$ values is of particular interest in describing strongly focused or

divergent beams. As kw_0 increases, the magnitude of the backscattering as well as the amplitude of the radiation force function increase.

To closely examine the conditions for which the nulls tend to appear (pointed by arrows in Fig. 3) in the plots, the components K_{qG}, U_{qG}, R_{qG} as well as Y_{qG} are evaluated through Eqs.(12)-(15) for kw_0 = 0.1. From Fig. 3, it is noticed that all the three components, namely the kinetic energy density, the potential energy density as well as the momentum flux density vanish simultaneously at the selected *ka* values for the nulls, unlike the case of the zero-force predicted for spherical waves on a rigid sphere (See Fig. 3 in [23], around ka = 3.9) for which both the kinetic energy density as well as the potential energy density have same magnitudes but opposite amplitudes. In addition, it is noticeable that for a tightly focused (or strongly divergent) quasi-Gaussian beam (i.e., $kw_0 \leq 1$), though the axial radiation force approaches closely to zero, it is not found to be negative (i.e. not a force of attraction), whereas for some situations, theoretical predictions have demonstrated the existence of a negative (pulling) force on a sphere placed in the close proximity of acoustical spherical waves [23-26], or in the field of focused Gaussian beams [27, 28], Bessel beams [29-32], plane waves on an elastic spherical shell close to a boundary [33], or plane waves on a coated sphere [16]. Complete acoustical tweezing requires immobilization of a particle in the acoustical field (i.e. producing a mean zero force). However, in practical cases, a pulling force may be required to counteract the effects of possible mechanical instabilities (e.g., hydrodynamic forces, viscous forces, etc.) that could destabilize the trap using a single beam. Further experiments using acoustical quasi-Gaussian beams are warranted to address this problem.

To analyze the behavior of the radiation force function and its density distribution along a selected direction θ, the kinetic, potential, momentum flux, and radiation force density functions are evaluated using Eqs.(20)-(23) for $kw_0 = 0.1$ at the zeros of Y_{qG} (pointed to by arrows in Fig. 3). The results are displayed in panels (a)-(d) of Fig. 4 for ka = 3.366, 4.806, 6.456 and 7.691, respectively. In all cases, all the density functions including $y_{qG}(\theta)$ exhibit an anti-symmetric behavior with respect to the direction $\theta/\pi =$ 0.5. From Fig. 4, one concludes that both anterior ($0 \le \theta/\pi \le 0.5$) and posterior ($0.5 \le \theta/\pi \le 1$) areas of the sphere experience a force of equal magnitude in opposite direction, resulting in a zero mean force on the sphere, at the selected ka values.

Viscoelasticity inside the sphere's material and its effect on the radiation force function for a quasi-Gaussian beam is further analyzed by introducing complex wave numbers into the theory [34-36]. The curves shown in Fig. 3 for the *elastic* sphere case, are now computed for a viscoelastic PMMA sphere, for which the plots for the components K_{qG}, U_{qG}, R_{qG} as well as Y_{qG} are shown in Fig. 5 for $kw_0 = 0.1$. For the first null that have occurred at ka = 3.366 for the elastic sphere case, the inclusion of absorption induces a slight shift to higher ka so that the first minimum in the plot for Y_{qG} occurs at ka = 3.406. Moreover, an increase in the kinetic K_{qG} and potential U_{qG} energy densities counteract the momentum flux density R_{qG}, giving birth to a positive (repulsive) force. The third null that have occurred at ka = 6.456 for the elastic sphere case (Fig. 3), becomes a minimum in the viscoelastic case that is shifted to lower ka = 6.406. As a general observation, comparison of Figs. 3 and 5 show that absorption *degrades* the zero-mean force. Initially, this behavior has been observed for the axial radiation force of a zero-order Bessel acoustical beam on a polyethylene viscoelastic sphere (see Fig. 8 in

Ref. [37]), and later discussed to include *vortex* beams by introducing the notion of acoustical efficiency factors [38].

Finally, additional computations are performed to examine the effect of varying kw_0 on the Y_{qG} curves. Fig. 6 shows the plots for a PMMA elastic sphere in water for $kw_0 = 5$, 10 and 25, respectively. As shown previously [11], when $kw_0 \geq 25$, the Y_{qG} plot closely approaches Y_p, where Y_p is the radiation force function for *plane waves* [36]. Fig. 6 shows that some resonances in the radiation force function curves tend to appear as kw_0 increases. To study this behavior, the magnitude of the backscattering form function $\left|f_\infty\left(ka, kz_R, \pi\right)\right|$ is plotted for the same set of parameters chosen for Fig. 6. Comparison of both figures show that the suppression of the resonance in the radiation force function curve of Fig. 6 around $ka = 5.336$ for $kw_0 = 5$, is associated with a reduction in the backscattering direction (Fig. 7). Moreover, the suppression of the Y_{qG}-resonances in Fig. 6 around $ka = 7.461$ and 8.876 for $kw_0 = 5$, is associated with a suppression of the scattering in the backward direction (Fig. 7). This behavior has also been observed in the context of Bessel beams [29]; that is a reduction of the scattering into the backward hemisphere reduces the radiation force.

Concerning the case where the sphere is shifted off-axis of the beam and the issue related to transverse stability, recent investigations based on the partial-wave expansion method [39], and utilizing the arbitrary scattering theory [40-43], have shed some light onto this topic for the case of Bessel beams [44, 45]. Those studies can be potentially extended to the case of quasi-Gaussian beams, and further experimental data is warranted to support the theoretical predictions and demonstrate the feasibility of particle tweezing.

Acknowledgments: The financial support provided through a Director's fellowship (LDRD-X9N9, Project # 20100595PRD1) from Los Alamos National Laboratory is gratefully acknowledged. Disclosure: this unclassified publication, with the following reference no. LA-UR 13-XXXXX, has been approved for unlimited public release under DUSA ENSCI.

Figures

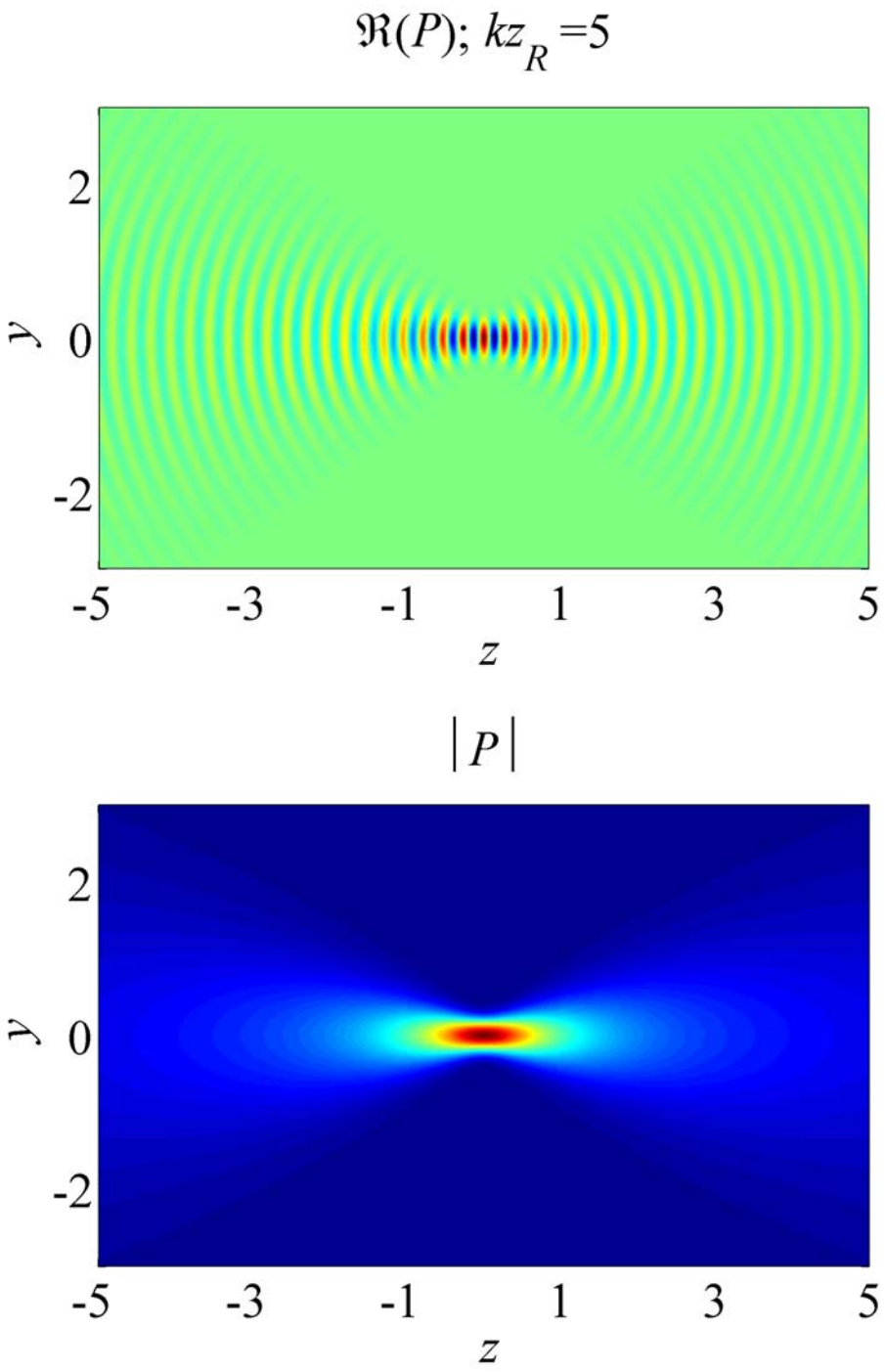

Fig. 1. (Color online) Instantaneous sound pressure (top panel) for a quasi-Gaussian beam at $kw_0 = 5$. The bottom panel represents the magnitude of the pressure for $k = 25$ m^{-1}. (See also the **Supplementary Animation**).

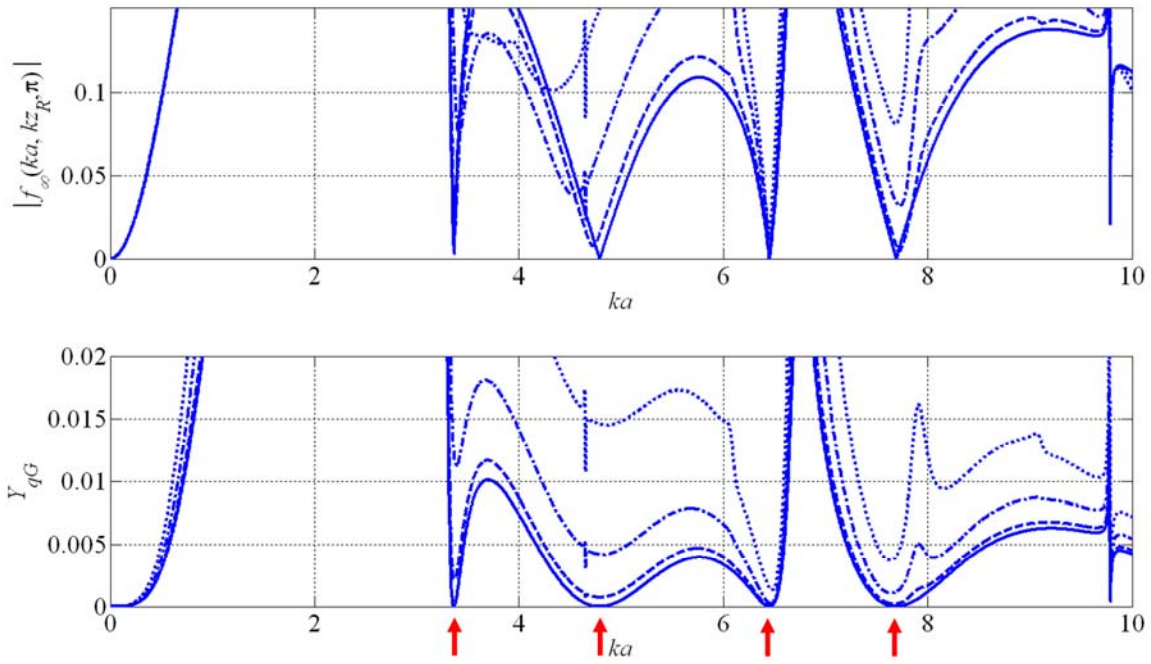

Fig. 2. (Color online) The plots for the backscattering form-function (top panel) and radiation force function (bottom panel), for a polymethylmetacrylate (PMMA) *elastic* sphere for $kw_0 = 0.1$ (solid line), $kw_0 = 1$ (long-dashed line), $kw_0 = 1.5$ (dashed-dotted line), and $kw_0 = 2$ (dotted line). The arrows along the ka axis in the bottom panel point to the zeros of Y_{qG} that occur at the minima-resonances of the elastic sphere.

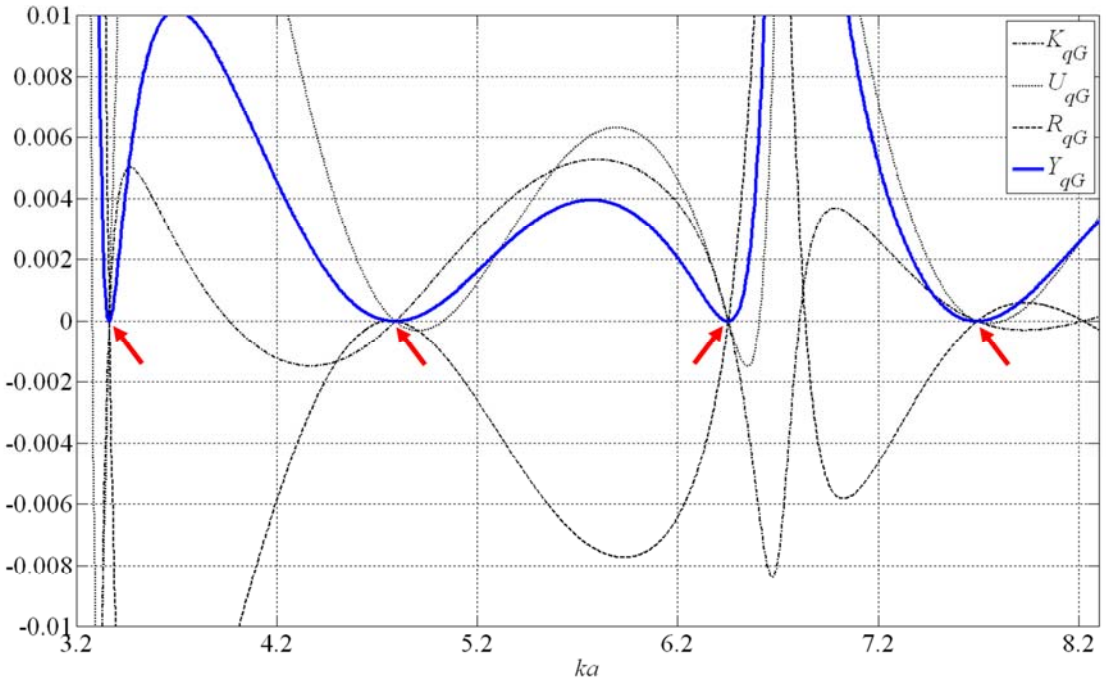

Fig. 3. (Color online) The plots for the the components K_{qG}, U_{qG}, R_{qG} as well as Y_{qG} for an *elastic* PMMA sphere for $kw_0 = 0.1$. It is noticed that all the three components, namely the kinetic energy density, the potential energy density as well as the momentum flux density vanish simultaneously at the selected *ka* values for the nulls.

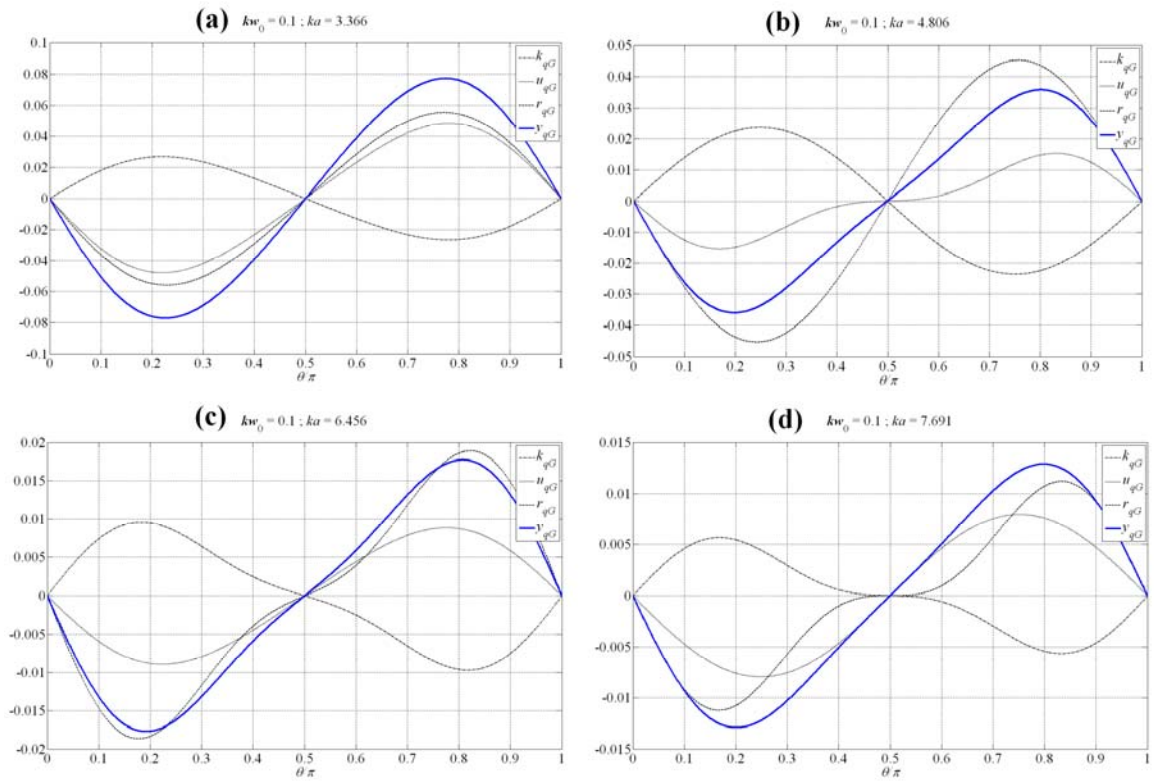

Fig. 4. (Color online) The plots for the density functions for an elastic PMMA sphere for kw_0 = 0.1 at the zeros of Y_{qG} (pointed to by arrows in Fig. 3). In all cases, all the density functions including $y_{qG}(\theta)$ exhibit an anti-symmetric behavior with respect to the direction $\theta/\pi = 0.5$.

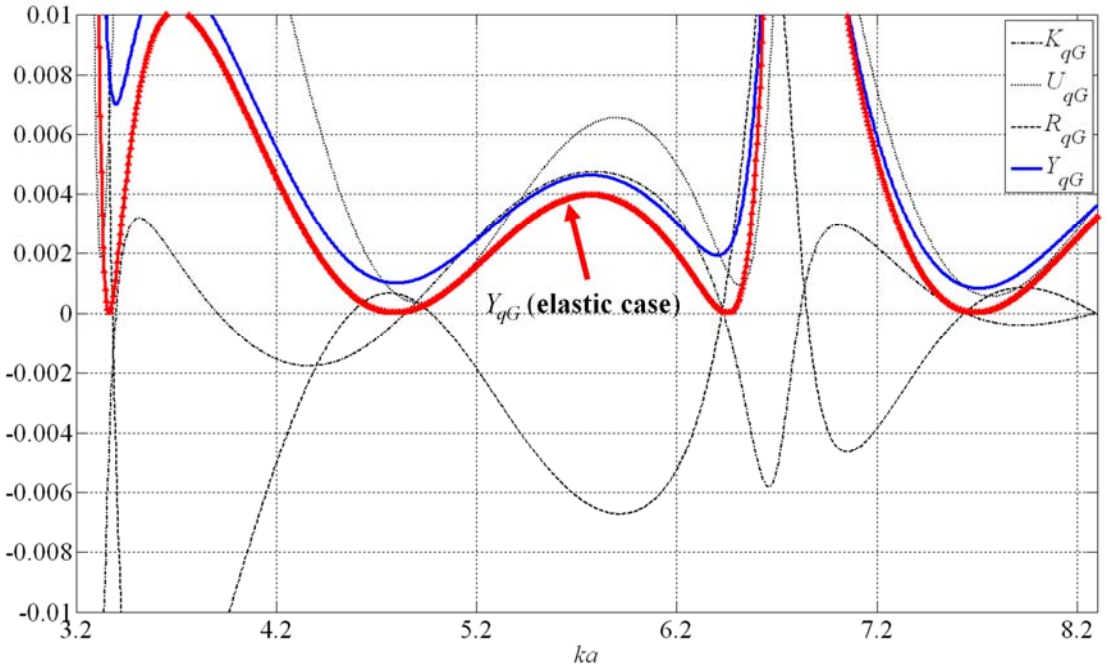

Fig. 5. (Color online) The same as in Fig. 3, however the PMMA sphere is *viscoelastic* (sound absorptive). The (red) curve with triangles (▲) corresponds to the case of no-absorption and is added for convenience.

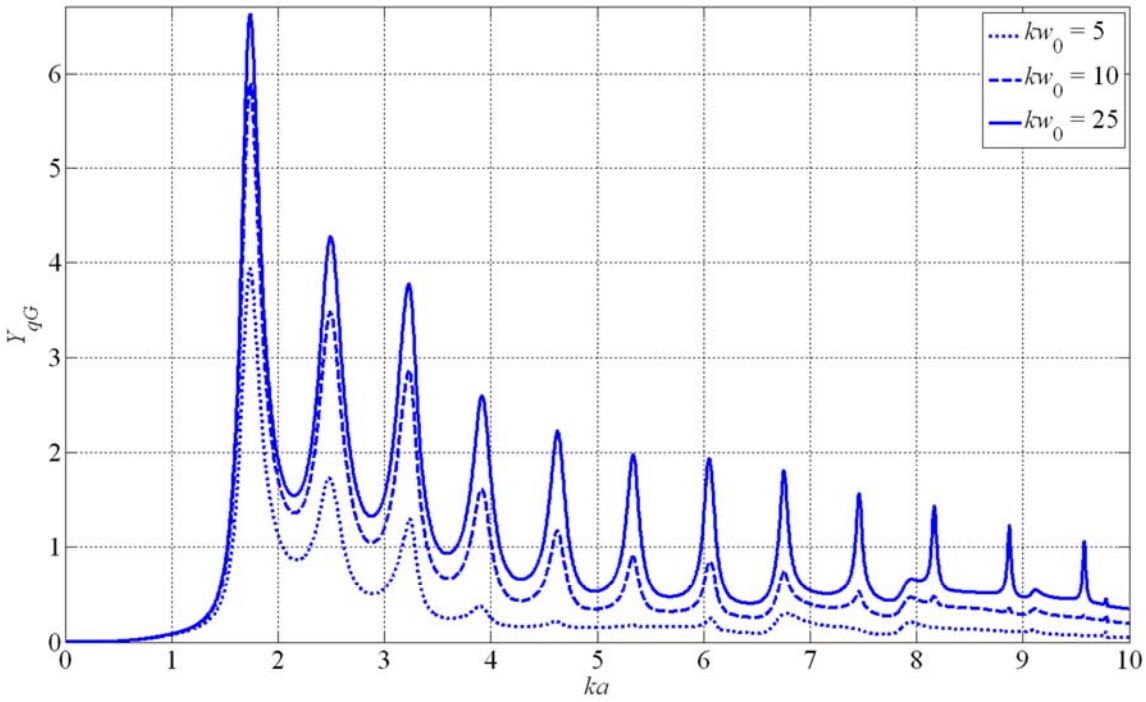

Fig. 6. (Color online) The Y_{qG} plots for a PMMA *elastic* sphere in water for kw_0 = 5, 10 and 25, respectively. The (quasi)plane wave limit is reached for ≥ 25.

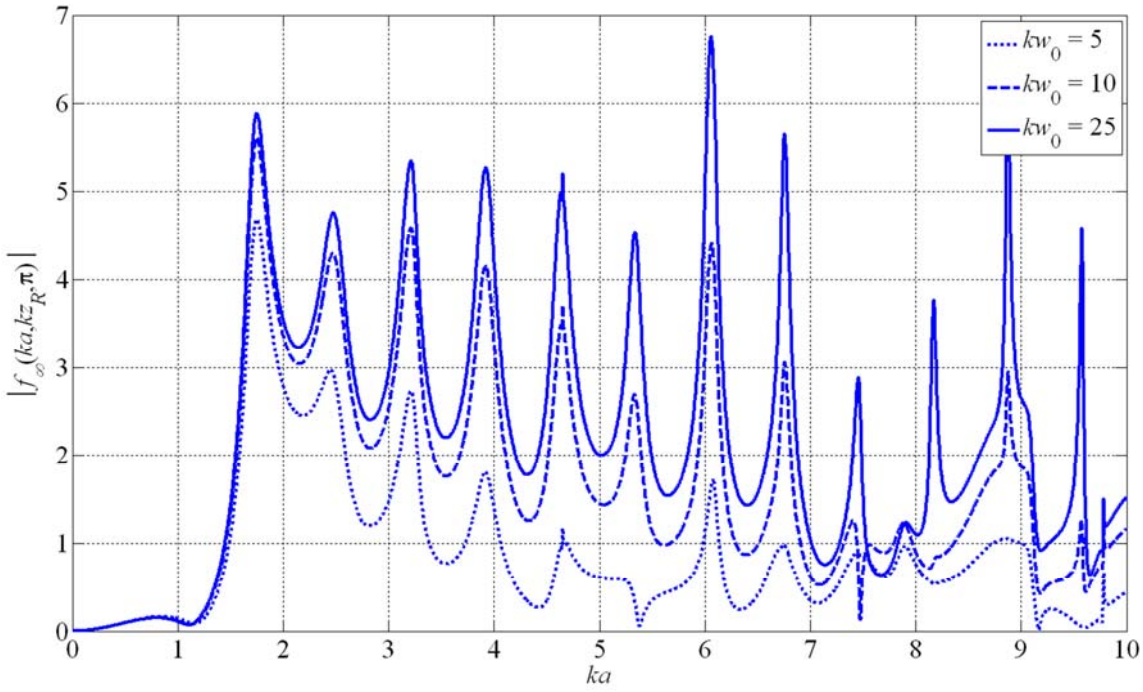

Fig. 7. (Color online) The magnitude of the backscattering form function $\left|f_\infty\left(ka, kz_R, \pi\right)\right|$ plots for $kw_0 = 5$, 10 and 25, respectively.

References

[1] J.B. Keller, J.F.C. Karal, Surface Wave Excitation and Propagation, J Appl Phys, 31 (1960) 1039-1046.

[2] G.A. Deschamps, Gaussian beam as a bundle of complex rays, Electron. Lett., 7 (1971) 684-685.

[3] J.B. Keller, W. Streifer, Complex Rays with an Application to Gaussian Beams, J. Opt. Soc. Am., 61 (1971) 40-43.

[4] L.B. Felsen, Evanescent waves, J. Opt. Soc. Am., 66 (1976) 751-760.

[5] M. Couture, P.A. Belanger, From Gaussian beam to complex-source-point spherical wave, Physical Review A, 24 (1981) 355-359.

[6] A.N. Norris, Complex point-source representation of real point sources and the Gaussian beam summation method, J. Opt. Soc. Am. A, 3 (1986) 2005-2010.

[7] A.N. Norris, T.B. Hansen, Exact complex source representations of time-harmonic radiation, Wave Motion, 25 (1997) 127-141.

[8] F.G. Mitri, Quasi-Gaussian electromagnetic beams, Physical Review A, 87 (2013) 035804.

[9] O.A. Sapozhnikov, An exact solution to the Helmholtz equation for a quasi-Gaussian beam in the form of a superposition of two sources and sinks with complex coordinates, Acoust Phys, 58 (2012) 41-47.

[10] M. Azarpeyvand, M. Azarpeyvand, Acoustic radiation force on a rigid cylinder in a focused Gaussian beam, J Sound Vib, 332 (2013) 2338-2349.

[11] F.G. Mitri, Interaction of an acoustical Quasi-Gaussian beam with a rigid sphere: linear axial scattering, instantaneous force, and time-averaged radiation force, IEEE Transactions on Ultrasonics, Ferroelectrics and Frequency Control, 59 (2012) 2347-2351.

[12] D.E. Chimenti, J.G. Zhang, S. Zeroug, L.B. Felsen, Interaction of Acoustic Beams with Fluid-Loaded Elastic Structures, J Acoust Soc Am, 95 (1994) 45-59.

[13] L. Schmerr, J.-S. Song, Ultrasonic Nondestructive Evaluation Systems: Models and Measurements, Springer, 2007.

[14] F.G. Mitri, Acoustic radiation force due to incident plane-progressive waves on coated spheres immersed in ideal fluids, Eur Phys J B, 43 (2005) 379-386.

[15] F.G. Mitri, Erratum to: Acoustic radiation force due to incident plane-progressive waves on coated spheres immersed in ideal fluids, The European Physical Journal B - Condensed Matter and Complex Systems, 76 (2010) 185-185.

[16] F.G. Mitri, Z.E.A. Fellah, The mechanism of the attracting acoustic radiation force on a polymer-coated gold sphere in plane progressive waves, European Physical Journal E, 26 (2008) 337-343.

[17] F.G. Mitri, Calculation of the acoustic radiation force on coated spherical shells in progressive and standing plane waves, Ultrasonics, 44 (2006) 244 -258.

[18] K. Yosioka, Y. Kawasima, Acoustic radiation pressure on a compressible sphere, Acustica, 5 (1955) 167-173.

[19] T. Hasegawa, K. Yosioka, Acoustic radiation force on a solid elastic sphere, J Acoust Soc Am, 46 (1969) 1139-1143.

[20] T. Hasegawa, T. Kido, C.W. Min, T. Iizuka, C. Matsuoka, Frequency dependence of the acoustic radiation pressure on a solid sphere in water, Acoustical Science and Technology, 22 (2001) 273-282.

[21] V.M. Ayres, G.C. Gaunaurd, Acoustic resonance scattering by viscoelastic objects, J Acoust Soc Am, 81 (1987) 301-311.
[22] A. Pierce, Acoustics: An Introduction to Its Physical Principles and Applications, Acoustical Society of America, 1994.
[23] T. Kido, T. Hasegawa, N. Okamura, Mechanisms for the attracting acoustic radiation force on a rigid sphere placed freely in a spherical sound field, Acoustical Science and Technology, 25 (2004) 439-445.
[24] T. Hasegawa, M. Ochi, K. Matsuzawa, Acoustic radiation pressure on a rigid sphere in a spherical wave field, J Acoust Soc Am, 67 (1980) 770-773.
[25] T. Hasegawa, M. Ochi, K. Matsuzawa, Acoustic radiation force on a solid elastic sphere in a spherical wave field, J Acoust Soc Am, 69 (1981) 937-942.
[26] X. Chen, R.E. Apfel, Radiation force on a spherical object in an axisymmetric wave field and its application to the calibration of high-frequency transducers, J Acoust Soc Am, 99 (1996) 713-724.
[27] J. Lee, K.K. Shung, Radiation forces exerted on arbitrarily located sphere by acoustic tweezer, J Acoust Soc Am, 120 (2006) 1084-1094.
[28] J. Lee, S.-Y. Teh, A. Lee, H.H. Kim, C. Lee, K.K. Shung, Single beam acoustic trapping, Applied Physics Letters, 95 (2009) 073701-073703.
[29] P.L. Marston, Axial radiation force of a Bessel beam on a sphere and direction reversal of the force, J Acoust Soc Am, 120 (2006) 3518-3524.
[30] F.G. Mitri, Langevin acoustic radiation force of a high-order Bessel beam on a rigid sphere, Ieee T Ultrason Ferr, 56 (2009) 1059-1064.
[31] F.G. Mitri, Negative Axial Radiation Force on a Fluid and Elastic Spheres Illuminated by a High-Order Bessel Beam of Progressive Waves, Journal of Physics A - Mathematical and Theoretical, 42 (2009) 245202.
[32] P.L. Marston, Radiation force of a helicoidal Bessel beam on a sphere, The Journal of the Acoustical Society of America, 125 (2009) 3539.
[33] A.K. Miri, F.G. Mitri, Acoustic Radiation Force on a Spherical Contrast Agent Shell Near a Vessel Porous Wall – Theory, Ultrasound in Medicine & Biology, 37 (2011) 301-311.
[34] L.S. Schuetz, W.G. Neubauer, Acoustic reflection from cylinders---nonabsorbing and absorbing, The Journal of the Acoustical Society of America, 62 (1977) 513-517.
[35] F.G. Mitri, Z.E.A. Fellah, J.Y. Chapelon, Acoustic backscattering form function of absorbing cylinder targets (L), J Acoust Soc Am, 115 (2004) 1411-1413.
[36] F.G. Mitri, Acoustic radiation force acting on absorbing spherical shells, Wave Motion, 43 (2005) 12-19.
[37] F.G. Mitri, Acoustic radiation force on a sphere in standing and quasi-standing zero-order Bessel beam tweezers, Annals of Physics, 323 (2008) 1604-1620.
[38] L.K. Zhang, P.L. Marston, Geometrical interpretation of negative radiation forces of acoustical Bessel beams on spheres, Phys Rev E, 84 (2011) 035601.
[39] G.T. Silva, An expression for the radiation force exerted by an acoustic beam with arbitrary wavefront (L), The Journal of the Acoustical Society of America, 130 (2011) 3541-3544.
[40] F.G. Mitri, G.T. Silva, Off-axial acoustic scattering of a high-order Bessel vortex beam by a rigid sphere, Wave Motion, 48 (2011) 392-400.

[41] G.T. Silva, Off-axis scattering of an ultrasound Bessel beam by a sphere, Ieee T Ultrason Ferr, 58 (2011) 298-304.
[42] F.G. Mitri, Generalized theory of resonance excitation by sound scattering from an elastic spherical shell in a nonviscous fluid, IEEE Transactions on Ultrasonics, Ferroelectrics and Frequency Control, 59 (2012) 1781-1790.
[43] F.G. Mitri, Arbitrary scattering of an acoustical high-order Bessel trigonometric (non-vortex) beam by a compressible soft fluid sphere, Ultrasonics, http://dx.doi.org/10.1016/j.ultras.2012.12.008 (2013).
[44] D. Baresch, J.-L. Thomas, R. Marchiano, Three-dimensional acoustic radiation force on an arbitrarily located elastic sphere, The Journal of the Acoustical Society of America, 133 (2013) 25-36.
[45] G.T. Silva, J.H. Lopes, F.G. Mitri, Off-axial acoustic radiation force of repulsor and tractor Bessel beams on a sphere Ieee T Ultrason Ferr, accepted - in press (2013).